Metabolism of ^{13}N-labeled Inorganic Nitrogen by Cyanobacteria and Higher Plants

C.P. Wolk, W.S. Chien, S.M. Austin, A. Galonsky, J.C. Meeks, J. Thomas, W. Lockau, T. Skokut, N. Schilling, P.W. Shaffer, and Y. Avissar

We have, in the past few years, developed methodology for generating N_2 and NH_4^+ highly labeled with ^{13}N and for determining the biochemical pathways by which these substances are metabolized. N_2 assimilated by specialized cells called heterocysts, in cyanobacteria, is reduced to NH_4^+ and the NH_4^+ incorporated into the amide group of glutamine in those cells. The glutamine is transported to vegetative cells, where the amide-^{13}N is in large part transferred to α-ketoglutarate to form glutamic acid[1]. The pathway NH_4^+ → glutamine → glutamate is the principal pathway for the assimilation of gaseous nitrogen by Anabaena cylindrica[2].

During the last year, we have applied these techniques to studies of the assimilation of NH_4^+ by vegetative cells of Anabaena cylindrica, of N_2 and NH_4^+ by a broad range of physiological types of other cyanobacteria, of NH_4^+ and, in preliminary experiments, of NO_3^- by tobacco cells in culture, and of N_2 by soybean nodules.

a) Assimilation of $^{13}NH_4^+$ by vegetative cells of Anabaena cylindrica. A. cylindrica grown in the presence of ammonium forms only, or nearly only, vegetative cells, and, as we had shown previously, these vegetative cells metabolize $^{13}NH_4^+$ predominately to glutamine amide-^{13}N. Glutamate also becomes labeled extensively after short periods of assimilation of $^{13}NH_4^+$. Four types of observations support the idea that glutamate is labeled principally by a reaction in series with, rather than in parallel with, glutamine formation. First, increasing the concentration of exogenous, stable NH_4^+ to 2 mM (a value approaching the saturation constant (K_m) of the glutamate dehydrogenase-catalyzed reaction for direct formation of glutamate from NH_4^+) has little effect on the relative rates of appearance of ^{13}N in glutamate and glutamine. Second, methionine sulfoximine and azaserine, inhibitors, respectively, of formation of and amide transfer from glutamine, greatly reduce the rate of formation of glutamate. Third, if extensive formation of glutamine takes place before the inhibition by methionine sulfoximine becomes fully effective, a transfer of ^{13}N from glutamine to glutamate is observed. Finally, when 3-s pulses of $^{13}NH_4^+$ are chased with 5 mM NH_4Cl, ^{13}N is transferred from the amide group of glutamine into glutamate and then, after a lag period, into the α-amino group of glutamine (see Fig. 1).

Formation of [^{13}N]aspartate is inhibited more than 90% by the presence of aminooxy acetate,

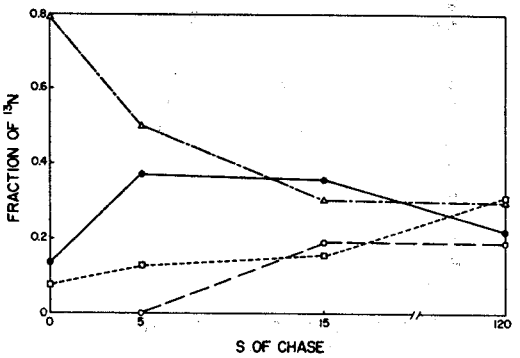

Fig. 1.--Time-course of the fractions of extractable ^{13}N in amide (Δ) and α-amino (□) groups of glutamine, and in glutamate plus aspartate (●) and other constituents (○), during a "chase" with 5 mM NH_4Cl after 3 s of assimilation of $^{13}NH_4^+$ by NH_4^+-grown Anabaena cylindrica in the absence of supplemental NH_4Cl. Glutamate plus aspartate, and total glutamine, were determined from scans of radioactivity from ^{13}N in electrophoretograms. The regions corresponding to glutamine were then eluted, and the fraction of ^{13}N in amide nitrogen determined by distillation in the presence of alkali. Non-distillable ^{13}N in the glutamine region was taken to be α-[^{13}N]amino nitrogen.

whereas formation of glutamine and glutamate is relatively little affected, implying that formation of aspartate is dependent upon a transamination reaction. The observations that ^{13}N appears more rapidly in citrulline than in arginine, and that the syntheses of [^{13}N]citrulline and [^{13}N]-arginine are extensively inhibited by methionine sulfoximine, azaserine, and aminooxy acetate are consistent with the ideas that arginine is derived from citrulline and that the formation of citrulline is dependent upon amide- and amino-transferase reactions. Aspartate and arginine, which are labeled early and extensively, can be copolymerized to form multi-L-arginyl-poly(L-aspartic acid), the principal nitrogenous reserve product of cyanobacteria.

b) Metabolism of [^{13}N]N_2 and $^{13}NH_4^+$ by a spectrum of physiological types of cyanobacteria. Our initial, extensive studies of the metabolism of [^{13}N]-N_2 and $^{13}NH_4^+$ were done using only Anabaena cylindrica, a filamentous cyanobacterium with intercalary (intra-filament) heterocysts. In order to determine whether or not other cyanobacteria metabolize inorganic nitrogen in the same way that Anabaena cylindrica does, we are examining the organic products of assimilation of [13N]N_2 and $^{13}NH_4^+$ by the following range of morphological and physiological types of cyanobacteria: (1) Anabaena variabilis, structurally very similar to A. cylindrica, but on which we are conducting intensive genetic

studies; (2) Cylindrospermum licheniforme, a filamentous species with heterocysts only at terminal positions; (3) Plectonema boryanum, a filamentous species lacking heterocysts, and which fixes N_2 only during growth at low partial pressures of O_2; (4) Gloeothece species, unicellular, lacking heterocysts, and capable of slow growth on N_2; and (5) Anacystis nidulans, unicellular, incapable of N_2 fixation, and used in many laboratories for studies of photosynthesis, intermediary metabolism, molecular biology, and genetics.

Our experiments on the filamentous species have essentially been completed. The initial organic product of fixation of $[^{13}N]N_2$ in all three species is glutamine. ^{13}N is then transferred to glutamate, which becomes more radioactive than glutamine after 60 to 120 s of fixation. After 120 s of assimilation, citrulline is highly radioactive in A. variabilis, whereas only glutamine and glutamate are conspicuous in the metabolic products of C. licheniforme and P. boryanum. Glutamine is also the initial organic product of assimilation of $^{13}NH_4^+$ in all three species, and glutamate the second major product. Methionine sulfoximine blocks formation of glutamate nearly as extensively as it blocks formation of glutamine. The ratio of $[^{13}N]$glutamate to $[^{13}N]$glutamate is >1 after 900 s of assimilation of $^{13}NH_4^+$ by P. boryanum, ∿1 after 900 s of assimilation of C. licheniforme, and <1 after 120 s of assimilation by A. variabilis. In all three species aspartate, citrulline, and/or alanine contain significant ^{13}N after 120 s, and ^{13}N is present in arginine within 900 s. Inhibition of formation of glutamine by methionine sulfoximine also inhibits formation of ^{13}N-labeled aspartate, citrulline, and arginine. Preliminary experiments with Anacystis nidulans indicate that the first product of assimilation of $^{13}NH_4^+$ is glutamine, and that the ratio of $[^{13}N]$ glutamate to $[^{13}N]$glutamine remains low. The identities of the ^{13}N-labeled amino acids formed by each species were established in part by two-dimensional radioscans following two-dimensional separations (electrophoresis followed by chromatography), using a newly developed, two-dimensional scanner described elsewhere in this report.

Our results to date support the conclusion that sequential formation of glutamine and glutamate by the enzymes glutamine synthetase and glutamate synthase is the principal pathway of assimilation of inorganic nitrogen by a diverse group of cyanobacteria. The other amino acids formed are to a large extent also dependent upon amide and amino transfer reactions from glutamine and glutamate. A difference in the kinetics of incorporation of ^{13}N into glutamine and glutamate, depending upon the source of nitrogen as N_2 or NH_4^+, implies that glutamine synthetase and glutamate synthase may be separated by compartmentation even in Plectonema boryanum, a species which lacks heterocysts. It will be of interest to ascertain whether such compartmentation also occurs in the colonial, N_2-fixing cyanobacterium, Gloeothece sp.

c) $[^{13}N]N_2$ fixation by detached root nodules of soybean. The most successful symbiotic N_2-fixing association, and currently the most important agronomically, occurs between bacteria of the genus Rhizobium and higher plants of the family Leguminosae. In this association, N_2 is fixed by the infecting, differentiated bacteria in nodules formed on the plant roots. The fixed nitrogen must then be translocated to the stems, leaves, and fruits for growth and development of the plant. One aspect of the development of high-yielding legume varieties involves genetic selection of the plants most successful in the fixation and translocation of nitrogen. Based on studies of translocation of ^{14}C-labeled compounds, analysis of amino acid pools, and preliminary ^{15}N tracer experiments, it has commonly been assumed that the amino acid asparagine functions as the major compound in the translocation of fixed nitrogen. In the development of high yielding varieties, it is important to know what the immediate products of N_2-fixation are in root nodules, and to establish firmly the identity of the transported nitrogenous compound and whether this compound is synthesized in the root nodule or the root proper. To this end, we have initiated experiments on $[^{13}N]N_2$ fixation in symbiotic associations of the bacterium Rhizobium japonicum and the legume Glycine max (soybean).

We are currently working with detached nodules, and the resulting data are of a most preliminary nature. We have not yet successfully observed $[^{13}N]N_2$ fixation for exposure times less than 60 s. However, after 60 s of fixation ^{13}N radioactivity is distributed nearly equally between glutamine and glutamate, with a trace of radioactivity detectable in alanine. After 360 s of fixation glutamate is the most highly labeled compound, followed by glutamine and then alanine. Glutamate remains the most highly labeled compound after 900 s of fixation, but more radioactivity is associated with alanine than with glutamine. Thus far, ^{13}N radioactivity has been detected only in those three amino acids at all fixation times with detached nodules. Thus, even after 900 s of fixation no ^{13}N radioactivity is associated with asparagine. It is possible that, if asparagine is the major compound involved in translocation of fixed nitrogen, it is synthesized in the root from one of the three initial organic products of N_2-fixation formed in the nodule. We have devised a method of exposing intact nodulated seedlings to $[^{13}N]N_2$ and hope to examine the synthesis and

transport of ^{13}N-labeled compounds in roots and stems.

d) Assimilation of [^{13}N]ammonium and [^{13}N]-nitrate by cultured tobacco cells. Tobacco (Nicotiana tabacum L. cultivar Xanthi) strain XD cells grown in liquid suspension culture form [^{13}N]-glutamine first and [^{13}N]glutamic acid second when fed [^{13}N]ammonium. The amounts of radioactivity in glutamine and glutamate increase with time, although glutamine always has the higher radioactivity, even after 10 minutes. Essentially identical results were obtained with cells grown on ammonium, nitrate, or urea as the sole nitrogen source. Methionine sulfoximine blocked incorporation of ^{13}N into glutamine by 88%, and azaserine inhibited incorporation of ^{13}N into glutamate by 95%. The above results suggest that ammonium is assimilated in these cells primarily via the pathway catalyzed by the enzymes glutamine synthetase and glutamate synthase.

[^{13}N]NO_3^- was generated by irradiation of a 1-ml sample of ^{16}O-enriched water with protons. The irradiated sample was found to contain varying amounts of [^{13}N]NO_3^-, [^{13}N]NO_2^- and [^{13}N]NH_4^+. The [^{13}N]NO_2^- was oxidized to [^{13}N]NO_3^- with 1.5% hydrogen peroxide. The [^{13}N]NH_4^+ was removed by raising the pH of the sample to pH 10 and evaporating the sample to dryness. Radioactivity from [^{13}N]NO_3^- was incorporated into amino acids in a manner similar to that found with [^{13}N]ammonia except that incorporation of ^{13}N into glutamine and glutamate was slower, and glutamate usually had a higher radioactivity than glutamine after 10 to 15 min of assimilation.

1. J. Thomas, J.C. Meeks, C.P. Wolk, P.W. Shaffer, S.M. Austin and W.S. Chien, J. Bact. 129(1977)1545-1555.
2. C.P. Wolk, J. Thomas, P.W. Shaffer, S.M. Austin and A. Galonsky, J. Biol. Chem. 251 (1976)5027-5034.

Production and Detection of ^{13}N Labeled NH_3, NO_3^-, NO_2^-, NO, N_2O and N_2 for Denitrification Studies

R.B. Firestone, M.K. Firestone, M.S. Smith, M.R. Betlach and J.M. Tiedje

The production of ^{13}N labeled NH_4^+, NO_3^-, NO_2^-, NO, N_2O and N_2 and their subsequent rapid separation and detection form the cornerstone of the denitrification studies currently in progress at the MSU Cyclotron Laboratory. The past year has shown rapid progress in the development of techniques for ^{13}N tracer experiments from the naive conception of experimental goals to the establishment of highly reliable procedures. In figures 1 and 2 we show clean separation of all six ^{13}N labeled species performed by various chromatographic techniques described in detail below.

^{13}N is produced by the $^{16}O(p,\alpha)^{13}N$ reaction utilizing either 12.7 MeV p beams or 25 MeV p beams degraded to 14.5 MeV by Al absorbers. 0.8 ml H_2O targets are bombarded with typically 1-3 μA beam currents for 10 minutes in a rapid retrieval rabbit system. Sources are nominally 1 mCi and contain primarily (85%) $^{13}NO_3^-$. Measurable amounts of ^{18}F produced by the $^{18}O(p,n)^{18}F$ reaction are also observed but do not affect the biology experiments. $^{13}NH_4^+$ is effectively removed by making the sample basic and evaporating to dryness, and $^{13}NO_2^-$ can be eliminated by heating with H_2O_2 at pH 3.0 following bombardment. Nearly pure samples of $^{13}NH_4^+$ may also be directly produced by the addition of ascorbic acid to the water before bombardment as was previously shown by Tilbury.[1]

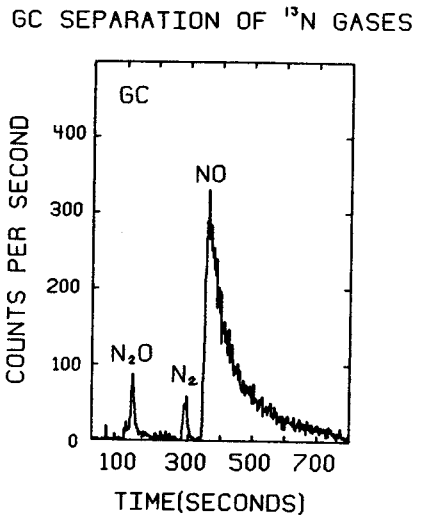

FIG. 1.--Gas chomotographic separation of gases.

Several different ^{13}N detection systems are available for various experimental requirements. A 2x2 inch NaI well counter with a 9/16" x 1½" well is used to count liquid source aliquots for absolute source activity measurements. Typically sources are diluted to 5 ml and 100 ml samples are counted to obtain absolute source intensity. This detection mode is used to monitor

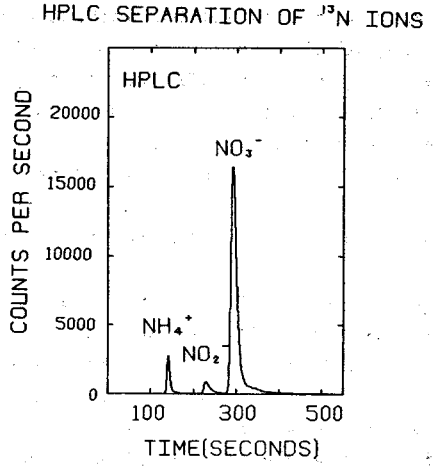

FIG. 2.--High performance liquid chromotographic separation of ions.

activity after various wet chemistry procedures have been used on the source or the biological products.

A continuous flow detection system has been used extensively to continuously monitor N_2O and N_2 production from soils. This system is an improved version of the one used by Gersberg, et al.[2] Besides improvements in the geometry and resolution, we are able to continuously monitor the N_2O and N_2 produced. A schematic of our incubation vessel and differential trapping system is shown in Figure 3.

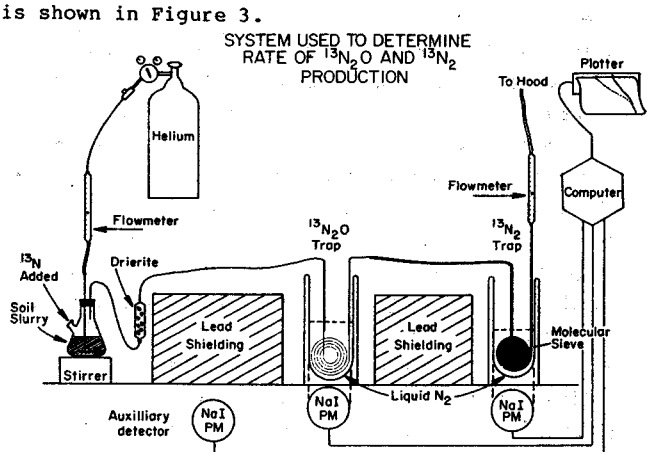

FIG. 3.--Continuous flow system.

In this type experiment a soil-water slurry is continuously mixed and the N_2+N_2O gases are stripped away by a continuous flow of He gas. This gas is then passed first through a liquid N_2 cooled trap where N_2O is deposited and finally through a liquid N_2 cooled Molecular Sieve trap which stops the N_2. Both traps are counted with 3x3 inch NaI(Tℓ) detectors. The pulses from these NaI(Tℓ) detectors, and the well detectors, are counted in CAMAC scalers interfaced to a PDP 11/45 computer. Here the scalers are read and recorded at arbitrary intervals, typically one minute, and the data is displayed both

numerically and graphically with corrections for half-life and background. The final corrected data is available immediately upon conclusion of the experiment allowing for instant analysis and planning of the subsequent experiment. The selectivity of this differential trapping system was shown by injecting $^{13}N_2$[3] and $^{13}N_2O$ (produced biologically and separated by gas chromotography) into the He flow. Approxiately 2.7% of the $^{13}N_2$ was observed in the first trap, while 1% of the $^{13}N_2O$ passed to the second trap.

A two column BASIC CARLE 8000 gas chromotograph (GC) is also used for separation and analysis of NO, N_2O and N_2 gases. With this system N_2O is separated from N_2 and NO by a PORAPAK N column through which the N_2 and NO pass quickly into a second 13x Molecular Sieve column which is in series with the first column. The He carrier gas flow is then diverted off of the second column allowing the N_2 and NO to be held there as long as desired. When the labeled N_2O comes off the first column it is detected by a flow-through, single-wire proportional counter of 25 cm^3 volume operating with a 60% propane--40% helium mixture. Upon detection of the N_2O the gas flow is switched back through the second column where N_2 and NO are separated and then counted with the proportional counter. A sample spectrum showing N_2O, N_2, and NO separated in this manner is shown in Figure 1. The GC detection system allows experiments with a large number of treatments in sealed flashes since the headspace is easily monitored over periodic intervals. In contrast the continuous flow system described above allows very short term and precise monitoring of the role of production of each gas and avoids the further reduction of any accumulated N_2O. The two methods are complimentary and thus allow important versatility in the possible types of denitrification experiments.

The separation of the NO_3^-, NO_2^- and NH_4^+ present in liquid samples is performed with a High Performance Liquid Chromotography system (HPLC).[4] A Partisil SAX column, operated at 800 lb/in^2, efficiently separates NH_4^+, NO_2^-, and NO_3^-. In Figure 2 the HPLC separation of all three components is shown for a typical, unpurified irradiated water sample. The effluent of the column is monitored by a dual 2x2 NaI coincidence counter which effectively suppresses background. The output of both the GC and HPLC detectors are counted in a multiscaler mode at the MSU Cyclotron Laboratory SIGMA-7 computer.

The techniques described here are now in routine operation. A great deal of new data about denitrification has now been obtained and it is already clear how significant these techiques can be. It should be emphasized that these studies cannot be performed by other methods and the developments discussed here represent a very unique experimental facility.

---

1. R.S. Tilbury, Personal communication, Memorial Sloan-Kettering Cancer Center.
2. R. Gersberg, K. Krohn, N. Peak, and C.R. Goldman, Science 192,1229(1976).
3. Prepared by the research group of Dr. Peter Wolk at the MSU Cyclotron Laboratory.
4. R.S. Tilbury, and J.R. Dahl, Abst. Rad. Res. Soc., 25th Annual Meeting, San Juan, Puerto Rico.

Short-term Studies of Denitrification Rates and Products using ^{13}N Labeled Nitrogenous Oxides

J.M. Tiedje, R.B. Firestone, M.K. Firestone, M.S. Smith and M.R. Betlach

Denitrification is the least understood process in the biogeochemical nitrogen cycle. This process is essentially the opposite of nitrogen fixation in that combined nitrogen (as nitrate) is reduced to the gaseous products, nitrous oxide or nitrogen, which are unavailable to biology. Denitrification is carried out by bacteria prevalent in soils and waters throughout the planet. The reductive sequence which occurs in denitrification is: $NO_3^- \rightarrow NO_2^- \rightarrow NO \rightarrow N_2O \rightarrow N_2$. Because denitrification results in a loss of nitrogen available to plants, there has been renewed interest in better understanding the process so that soil and fertilizer nitrogen can be better conserved. It is estimated that world nitrogen losses by denitrification are five times greater than total world fertilizer production. Thus, control of this process has the potential to be as significant to food productivity as would be the projected advances from research on nitrogen fixation. In addition to the goal of conserving nitrogen, recent concern over the denitrification intermediates, nitrous oxide and nitrite has surfaced. The former catalyzes destruction of the ozone layer through its photochemical product, nitric oxide, and the latter reacts with secondary amines to form nitrosamines which are potent carcinogens.

Despite the general importance of this process, progress in understanding denitrification in nature has been stymied by the absence of direct and sensitive methods to quantify denitrification rates and products. Short-term rate measurements--essentially enzyme assays--hold the greatest promise for new breakthroughs in understanding since these would allow the elucidation of direct cause and effect relationships between environmental parameters, which can change hourly, and the actual rate of denitrification. Previous work has been done with ^{15}N but the limited sensitivity and high isotope concentrations required make it impossible to determine the natural rate. During the past year, we have examined the feasibility of using ^{13}N-nitrate for studying denitrification and have obtained basic new information on the process.

a. Rates and Temporal Pattern of Denitrification

Prior to our work denitrification rates in natural soil could not be detected until 12 hours or more had elapsed and even then amendments to soil were often necessary to achieve detectable results. Using ^{13}N-nitrate and the continuous flushing system, we can determine rates of gas production within minutes after starting the experiment. An example of the denitrification rate data for the two gaseous products is shown in Figure 1. We have also

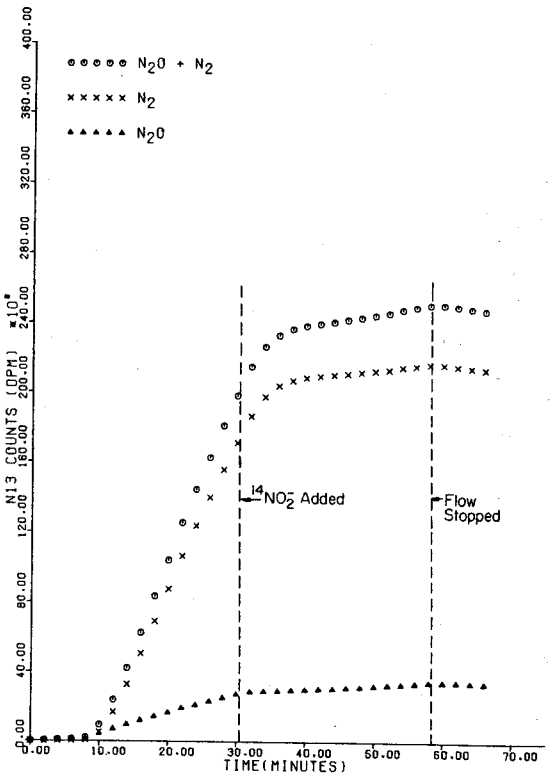

FIG. 1.--^{13}N gases produced after the onset of anaerobic conditions at -5 min. At 31 min. 20 ppm NO_2^--N was added to dilute the specific activity of the NO_2^- pool and at 58 min. the flushing gas was stopped. Data corrected for half-life and background.

been able to describe two linear phases in this earlier unknown period of denitrification. Phase 1 occurs in the first one to three hours (depending on soil); this rate reflects the enzyme activity of the soil at the time of collection. Following a transition period there is a second linear phase which appears to be due to derepression of denitrifying enzyme synthesis in the native population. The third phase, which may or may not be present depending on the soil, occurs after 12 to 24 hours and represents growth. The existence of phase 1 and 2 is also taken as evidence that denitrifying enzymes exist in common agricultural soils but that the activity is not fully induced. The latter point is particularly important since it means that methods to control denitrification could be based on control of derepression.

We have studied four soils which vary widely in properties and have obtained denitrification rates and the ratio of N_2O/N_2 for each in phase 1 and 2. For a typical midwest agricultrual soil (Brookston loam) the phase 1 rate was 0.51 nmol $N_2O \cdot g$ dry $soil^{-1} \cdot min^{-1}$ and the ratio of $N_2O/(N_2O+N_2)$ was 0.05. In phase 2 the rate had increased to 0.70 nmol $N_2O \cdot g$ dry $soil^{-1} \cdot min^{-1}$ and the product ratio had greatly increased to 0.34.

Mechanisms Causing N_2O Production

N_2O is often observed as an intermediate product of denitrification, yet factors which cause this break in the reductive sequence are not known. It is known that the N_2O in our atmosphere (approximately 300 ppb) is due to denitrification. Because of the recent concern over the N_2O effect on the ozone layer and the impact of increased fertilizer usage, we are attempting to answer basic questions on mechanisms causing N_2O production. We have shown that N_2O is a freely diffusible intermediate from cells. Increasing concentrations of $^{14}N_2O$ were added to soil denitrifying ^{13}N-nitrate. The amount of $^{13}N_2O$ produced increased with increased $^{14}N_2O$ added. Thus internal and external pools of N_2O are freely exchangeable. This finding means that any mechanism which causes a reduction in rate of a step subsequent to N_2O or an increase in rate of steps preceeding N_2O would cause N_2O to accumulate and thus be emitted from the cells.

We have established three hypotheses, all with supporting data, which seem to account for enhanced N_2O production. First, the temporal pattern of denitrification has consistently shown that the proportion of N_2O:N_2 produced increases with time after the onset of anaerobiosis for the first day. Thereafter the ratio shifts to nitrogen being the major product. This suggests that there is some difference in rate of synthesis or activation of the different enzymes in the reductive pathway. An example of this shift can be seen by comparing Figure 1 with Figure 2. The soil which provided the data for Figure 1 was anaerobic for only 5 minutes while the soil which provided the data for Figure 2 was anaerobic for 8 hours. In the latter case over 90% of the denitrification product was N_2O. It is felt that in nature that periodic rainfalls, which reduce oxygen availability, might produce an analogous response.

Secondly, the presence of competing electron acceptors, i.e. nitrate, nitrite, oxygen, may divert the flow of electrons from nitrous oxide reduction to the reduction of the above molecules. We have found that when the concentration of nitrate is increased that there is a corresponding increase in the N_2O:N_2 ratio, thus supporting the second hypothesis. We have found that nitrate concentrations as low as 0.5 ppm nitrate-N will cause a significant enhancement in N_2O production. This example points to the value of the ^{13}N method since this concentration is in the range found in nature but is not amenable to experimentation with any other method since the quantity of products would be below the detection limits.

As a third hypothesis we have preliminary evidence that carbon availability, probably expressed as electron donor, also effects the ratio of the two gaseous products.

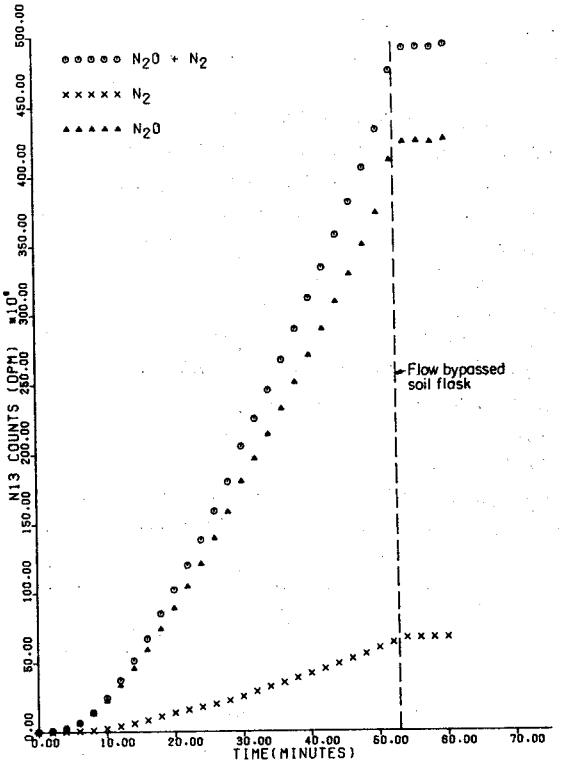

FIG. 2.--^{13}N gases produced after 8 hours of anaerobic incubation prior to adding $^{13}NO_3^-$. At 52 min. the gas flow was routed to bypass the soil flask to confirm that the ^{13}N gases did not migrate from their respective traps. Data corrected for half-life and background.

c. Experiments on Nitric Oxide Exchange

The denitrification intermediate, NO, has rarely been observed and is presumed to be enzyme bound. We have re-examined this question with the more sensitive ^{13}N methodology. When increasing amounts of ^{14}NO were added to soils denitrifying ^{13}N-nitrate, ^{13}NO was observed. However, the production of this free radical was also observed in sterilized soil in a similar experiment. It is felt that the NO is being produced from the destruction of HONO which could be catalyzed by mineral surfaces, H^+ and/or Fe^{+2}.

We feel that the greatly improved sensitivty that ^{13}N has provided will continue to allow us to probe for understanding the basic mechanisms and rates of denitrification. In the future we plan to develop experimental systems which would allow us to work with undisturbed soil cores and with an intact soil-plant system. It is postulated that denitrification is most significant in the zones surrounding plant roots, a hypothesis that has been impossible to test. By devising a system in which we can monitor ^{13}N assimilated into the plant and ^{13}N emitted as gases from the soil we should be able to determine the partitioning of nitrate between these two competing processes. This should provide us with fundamental new insight into how effectively different plants compete for their most limiting nutrient

Tantalum-178 - A New Shortlived Radionuclide for Medical Imaging: Production of ^{178}W

Gale I. Harris, Peter Miller, W.S. Chien, B. Leonard Holman, Alun G. Jones, John Idoine and Rudi D. Neirinckx

Recently work has been carried out on a number of alternatives or modifications to present gamma camera systems which appear to offer improved imaging capabilities. For example, the high-pressure multiwire proportional camera (MWPC) promises to provide high spatial resolution and an ability to accept count rates more than twice those of present detectors.[1] The Fresnel zone plate coded aperture system offers an alternative collimation technique which can in principle be applied to any kind of detection system and may also provide high spatial resolution and high efficiency. Both concepts, however, are better suited to low energy radiation emitters. For example, the MWPC has an efficiency of 25% at 140 keV, 70% at 80 keV and 80% at 60 keV. This report describes a production of the radionuclide ^{178}Ta, which shows promise for such systems.

^{178}Ta is formed in the decay of its parent ^{178}W (half-life 21.7 d), decaying with a half-life of 9.3 min to stable ^{178}Hf. 99.2% of the disintegrations proceed by electron capture and 0.81% by positron emission.[2] Electron capture results in 61.2% branch to the ground state of the stable product and 33.7% to the first excited state at 93.1 keV. The balance (4.3%) feeds levels between 1175 and 1772 keV. The gamma ray spectrum of the radionuclide is dominated by hafnium characteristic radiation with energies between 54 and 65 keV.

The reaction chosen was $^{181}Ta(p,4n)^{178}W$. Preliminary calculations based on the nuclear evaporation code ALICE[3] predicted an energy-dependent cross section approximately Gaussian in shape centered at about 34 MeV with a full width at half maximum of 10 MeV and 2200 mb at maximum. By comparison, the two strongest competing reactions at 34 MeV are $^{181}Ta(p,5n)^{177}W$ and $^{181}Ta(p,3n)^{179}W$ with cross sections lower than (p,4n) by factors of 11 and 60, respectively. Thus optimal conditions should be met at 34 MeV to achieve maximum ^{178}W production while avoiding that of ^{177}W. The latter decays to ^{177}Hf via ^{177}Ta ($t_{1/2}$ = 57h) giving rise to a 113-keV gamma ray in ^{177}Hf.

With these calculations as a guide, five 0.005-inch-thick tantalum foils mounted in a pneumatic rabbit assembly were irradiated at an incident proton energy of 40 MeV with a beam loss of 8 MeV in the target.

Gamma-ray spectra were obtained using a Ge(Li) detector approximately 30 hours after bombardment, when most short-lived activities were negligible. Maximum yields of ^{178}W activity occurred at about E_p = 35 MeV in reasonable agreement with the evaporation model estimates. The 113 keV gamma ray from the decay product of ^{177}W decreased rapidly in intensity with decreasing beam energy, varying from 2.4 times the intensity of the 93 keV peak at E_p = 39 MeV to 0.16 at E_p = 36. At E_p = 35 MeV and below, it was practically negligible.

The dominant features of the spectrum are the intense tantalum and hafnium characteristic radiations following the electron capture decay of ^{178}W and ^{178}Ta respectively. Tantalum K_α and K_β lines are seen at 56-58 and 65-67 keV, and hafnium K_α and K_β lines at 54-56 and 63-65 keV. The intensity of the 93 keV peak in the decay of ^{178}Ta is approximately twelve times lower than the K-Xray intensities. Furthermore, the transition is 83% internally converted, leading to an effective incidence of 6.3% per ^{178}Ta disintegration. A production rate of approximately 1.1 mCi/μA-hr per MeV of target thickness is inferred from these figures.

In order to separate out ^{178}W, the irradiated portions of the tantalum foils were cut out and dissolved in concentrated Hf containing nitric acid. The solution was evaporated to dryness, treated with concentrated HCl and again evaporated to dryness. The residue was dissolved in 6N HCl - 1.5M HF solution and eluted through a pre-equilibrated Bio-Rad AG 1x8 (200-400 mesh) anion exchange column. Separation of the equilibrium mixture from the tantalum target was accomplished with a yield of 98%.

The short-lived radionuclide ^{178}Ta has physical decay characteristics which could lend themselves to use of the isotope in diagnostic nuclear medicine. Furthermore, the half-life of the parent ^{178}W(21.7 d) is such that this nuclide could form the basis of a generator system for its short-lived product. An important point to note is that decay of ^{178}W does not feed the high spin level in ^{178}Ta ($t_{1/2}$ = 2.2h), nor in turn does ^{178}Ta decay populate the 4.3 second isomeric state at 1148 keV in ^{178}Hf.[2] Only the 9.3-m state is observed.

This work demonstrates that ^{178}W can be readily produced in both the quality and purity demanded in diagnostic nuclear medicine using simple target techniques. The optimal average proton energy in the target has been determined to be about 35 MeV at which energy the (p,5n) product ^{177}W is negligible.

The primary application of the radionuclide would appear to be in imaging the heart since this

is not a deep-seated organ and can be closely approached by an external detector. Coupled with the high sensitivity (80%) of the MWPC at the energies of the hafnium characteristic radiation, tissue absorption of the emissions may be sufficiently offset to warrant further investigation of this use. In first-pass radioangiocardiography high data rates are required over a short period of time. Large doses of a short-lived radionuclide could be administered, thereby allowing a more accurate assessment of regional wall motion abnormalities and regional cardiac hemodynamics. Of equal importance, multiple studies could be performed at reasonable intervals under physiologically or pharmacologically altered conditions because of the short half-life of the radiotracer.

---

1. S.N. Kaplan, L. Kaufman, V. Perez-Mendez and K. Valentine, Multiwire Proportional Counters for Biomedical Application. Nucl. Inst. & Meth. 104, 397 (1973).
2. C.M. Lederer, J.M. Hollander and I. Pearlman (eds.), Table of Isotopes, 6th Ed., John Wiley & Sons, Inc. (1968).
3. M. Blann and F. Plasil, ALICE: A Nuclear Evaporation Code. A modified version of the BSX evaporation code.